Role of Zymogenicity-Determining Residues of Coagulation Factor VII/VIIa in Cofactor Interaction and Macromolecular Substrate Recognition†

Ramona J. Petrovan and Wolfram Ruf*

Department of Immunology, The Scripps Research Institute, La Jolla, California 92037

Received March 19, 2002; Revised Manuscript Received May 30, 2002

ABSTRACT: Factor VIIa (VIIa) remains in a zymogen-like state following proteolytic activation and depends on interactions with the cofactor tissue factor (TF) for function. Val^{21}, Glu^{154}, and Met^{156} are residues that are spatially close in available zymogen and enzyme structures, despite major conformational differences in the corresponding loop segments. This residue triad displays unusual side chain properties in comparison to the properties of other coagulation serine proteases. By mutagenesis, we demonstrate that these residues cooperate to stabilize the enzyme conformation and to enhance the affinity for TF. In zymogen VII, however, substitution of the triad did not change the cofactor affinity, further emphasizing the crucial role of the activation pocket in specifically stabilizing the active enzyme conformation. In comparison to $VIIa_{Q156}$, the triple mutant $VIIa_{N21I154Q156}$ had a stabilized amino-terminal Ile^{16}−Asp^{194} salt bridge and enhanced catalytic function. However, proteolytic and amidolytic activities of free VIIa variants were not concordantly increased. Rather, a negatively charged Asp at position 21 was the critical factor that determined whether an amidolytically more active VIIa variant also more efficiently activated the macromolecular substrate. These data thus demonstrate an unexpected complexity by which the zymogenicity-determining triad in the activation pocket of VIIa controls the active enzyme conformation and contributes to exosite interactions with the macromolecular substrate.

Allosteric activation of coagulation factor VIIa (VIIa)[1] is a complex process that subjects the initiation of the coagulation cascade under functional regulation by VIIa's cell surface receptor and catalytic cofactor tissue factor (TF) (*3*). Cleavage of the Arg^{15}−Ile^{16} peptide bond[2,3] of serine protease zymogens typically leads to the formation of an internal salt bridge between Ile^{16} and Asp^{194} and to spontaneous ordering of the activation domain that is required for catalytic activity (*4*). In contrast, VIIa retains a zymogen-like conformation, as evidenced by low catalytic activity and an incompletely buried amino-terminal Ile^{16}. Binding to TF completes the transition of the VIIa protease domain to a catalytically active conformation (*1, 5*).

The structure of zymogen VII in complex with a peptide exosite inhibitor (*6*) shows a partially disordered "activation domain" in comparison to structures of VIIa that are active site modified and thus represent the transition state conformation (*7*−*11*). However, several structural features of VII are strikingly different from other zymogen structures of trypsin-like serine proteases. The primary specificity-determining Asp^{189} is flipped outward from the expected buried position seen in all VIIa structures (*7*−*11*). This is due to a three-amino acid shift in registration of β-strand B2 (residues 153−162) relative to complementary β-strand A2 (residues 134−140), which distorts the TF-binding helix with Met^{164}, a crucial TF-binding residue (*12*) that would not be properly positioned relative to TF unless the strand shift was reversed. However, the same protease domain residues are contributing to the interactions of the zymogen VII or enzyme VIIa with TF, and both, VII and VIIa, display similar TF binding kinetics (*12*−*15*). This indicates either that the zymogen and enzyme share the structural features of the distorted Met^{164} helix or that other conformations of VII exist in the fluid phase that do not interfere with the assembly of the protease domain with the cofactor.

VIIa has a triad of unusual residues (positions 21, 154, and 156) in the activation pocket that remain spatially close to each other in both the zymogen and enzyme structures, despite major conformational reordering of the respective loop segments (Figure 1). We have previously shown that mutation of one of these residues, Met^{156} to Gln (*16*), significantly increased the activity of free VIIa, and conversion of the entire three-residue motif to a mutant that mimics thrombin, $VIIa_{D21V154Q156}$ (*17*), further increased catalytic activity. It remained, however, unclear whether the improved function of the side chain replacement mutants resulted from a destabilized zymogen or a more stabilized enzyme conformation.

† This work was supported by National Institutes of Health Grant HL48752.

* To whom correspondence should be addressed: Department of Immunology, C204, The Scripps Research Institute, 10550 North Torrey Pines Rd., La Jolla, CA 92037. Telephone: (858) 784-2748. Fax: (858) 784-8480. E-mail: ruf@scripps.edu.

[1] Abbreviations: VII/VIIa, coagulation factor VII/VIIa; TF, tissue factor; PCPS, phosphatidylcholine/phosphatidylserine; sTF, soluble extracellular domain of TF, TF_{1-218}; X/Xa, coagulation factor X/Xa; CHO, Chinese hamster ovary cells; CHAPS, 3-[(3-cholamidopropyl)-dimethylammonio]-1-propanesulfonate; HBS, Hepes-buffered saline; TBS, Tris-buffered saline.

[2] Residue positions are numbered according to the chymotrypsin scheme described in ref *1*.

[3] S denotes subsite numbering according to Schechter and Berger (*2*).

10.1021/bi0202169 CCC: $22.00
Published on Web 07/04/2002

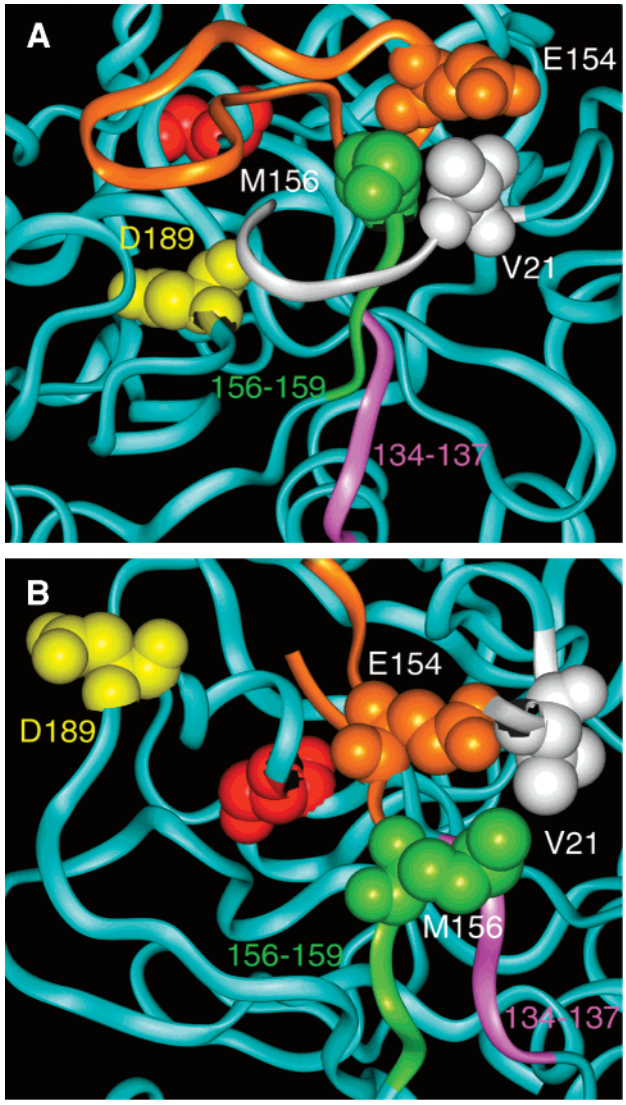

FIGURE 1: Structural comparison of enzyme VIIa with zymogen VII. The backbone is shown as a ribbon, colored to highlight the following segments: residues 16−22 (white), residues 134−137 (purple), residues 140−155 (orange), and residues 156−159 (green). Zymogenicity-determining residues 21, 154, and 156, the S1 specificity-determining residue Asp^{189} (yellow), and Ser^{195} (red) are shown in a surface representation. Similar views of the enzyme (A) (*10*) and the zymogen (B) (*6*) structures are shown.

In this study, we provide an extensive mutational analysis of this unique residue triad of VIIa. The data presented here demonstrate a cooperative effect of these residues in stabilizing the active conformation of VIIa, but not of zymogen VII. Moreover, the allosteric stabilization of the catalytic cleft by these mutations was separable from effects on improved macromolecular substrate activation that was most prominent in the absence of TF. In particular, the charge property of residue 21 was found to be the major determinant for the efficacy of macromolecular substrate activation. These experiments thus reveal unexpected complexity by which the activation pocket controls catalytic activity and extended substrate recognition.

EXPERIMENTAL PROCEDURES

Proteins. Recombinant wild-type and mutant factor VII were expressed in Chinese hamster ovary (CHO) cells and immunoaffinity purified using a calcium-dependent monoclonal antibody followed by anion-exchange chromatography, to select for γ-carboxylated protein, as previously described (*18*). Part of the protein was set aside to characterize the zymogen forms, and the remaining VII was converted >95% to the active enzyme by autoactivation at 4 °C in 20 mM Tris-HCl, 100 mM NaCl (pH 8.5), and 2 mM $CaCl_2$. Full-length recombinant human TF was produced from insect cells (*19*) and reconstituted with a 30% phosphatidylserine/70% phosphatidylcholine mixture (TF/PCPS) (*20*, *21*). The soluble extracellular domain of TF (sTF) was expressed in *Escherichia coli* and refolded from inclusion bodies (*22*). Plasma X was purified according to Fair et al. (*23*), followed by immunoaffinity chromatography as described previously (*1*). Protein concentrations were determined by the bicinchoninic acid assay (Pierce Chemical Co.) and converted to molar concentrations on the basis of calculated molecular masses.

VII mutants were generated by oligonucleotide-directed mutagenesis of the VII/pED4 construct as described previously (*1*). Introduction of all mutations was confirmed by DNA sequencing. Mutated proteins were expressed in CHO cells using transient transfection with the GenePorter-Reagent (GTS Systems). Cells were maintained in serum-free medium for 48 h to collect VII-containing supernatant which was concentrated and buffer-exchanged to 20 mM Tris-HCl, 100 mM NaCl (pH 8.5), and 250 μM $CaCl_2$ with an Ultrafree-15 centrifugal device (Millipore). The concentration of the recombinant protein was analyzed by ELISA (*1*). Conversion to the active enzyme by incubation with factor IXa at 37 °C (*24*) was confirmed by Western blot analysis with the monoclonal antibody F5-13B12.

Functional Characterization. Kinetic parameters for chromogenic substrate hydrolysis (Chromozym tPA, Roche) were determined at a fixed enzyme concentration (60 nM in the absence of TF or 30 nM in the presence of 120 nM sTF) with varying concentrations of substrate (from 20 μM to 2 mM) in Tris-buffered saline [TBS, 20 mM Tris and 150 mM NaCl (pH 8.0)], 5 mM $CaCl_2$, and 0.2% bovine serum albumin at ambient temperature. Initial rate data were fitted to the Michaelis−Menten equation using least-squares regression analysis. Amidolytic function of transiently expressed VIIa variants (5 nM) was assessed in the absence of TF with 0.7 mM Chromozym tPA in the same buffer at ambient temperature.

Kinetic parameters for X activation were determined at 37 °C, using a fixed concentration of TF/PCPS (200 pM) with 1 nM wild-type or mutant VIIa in Hepes-buffered saline [HBS, 10 mM Hepes and 150 mM NaCl (pH 7.4)], 5 mM $CaCl_2$, and 0.2% bovine serum albumin. X (from 8 nM to 1 μM) was added; samples were quenched with 100 mM EDTA, and Xa was quantified with the chromogenic substrate Spectrozyme FXa (American Diagnostics, Greenwich, CT). On the basis of calibration curves made with purified Xa, initial rates of Xa generation were calculated and fitted to the Michaelis−Menten equation using least-squares regression analysis. For the determination of the proteolytic activity of free VIIa, 20 nM wild-type or mutant VIIa was incubated for 30 min with 1 μM X in the presence or absence of 100 μM PCPS followed by assessment of Xa generation by a chromogenic assay.

Transiently expressed VII variants were analyzed in a functional assay at 37 °C in HBS, 5 mM $CaCl_2$, and 0.2%

bovine serum albumin to determine the affinity for TF and the maximal rate of Xa generation as a measure of proteolytic activity at saturation. A fixed concentration of TF/PCPS (5 pM) was saturated with increasing concentrations of VIIa, followed by assessing activation of 50 nM X to Xa. Rates of Xa generation versus the VII concentration were fitted to a single-site binding equation using least-squares regression analysis. To measure the proteolytic efficiency of the transiently expressed VIIa variants in the absence of TF, 10 nM mutant or wild-type VIIa was incubated with 1 μM X for 20 min at 37 °C in HBS, 5 mM $CaCl_2$, and 0.2% bovine serum albumin and Xa generation was monitored with Spectrozyme FXa.

Inhibition with p-Aminobenzamidine. The K_i for inhibition of VIIa with *p*-aminobenzamidine was determined in HBS, 5 mM $CaCl_2$, and 0.2% bovine serum albumin at a fixed wild-type or mutant VIIa concentration (60 nM in the absence of TF or 30 nM in the presence of 120 nM sTF). After a brief preincubation, 8 μM to 1 mM *p*-aminobenzamidine was added and the rates of hydrolysis of 0.7 mM Chromozym tPA were immediately determined in a kinetic microtiterplate reader. The apparent K_i values were calculated by fitting the data to a model for competitive inhibition at a fixed substrate concentration, taking into account the calculated parameters for chromogenic substrate hydrolysis.

Carbamylation of the α*-Amino Group in VIIa.* Wild-type or mutant VIIa (4 μM) or VIIa (1 μM) in complex with sTF (4 μM) was reacted with 0.2 M KCNO in HBS and 5 mM $CaCl_2$ at ambient temperature according to the method of Higashi et al. (*25*). After chemical modification for various amounts of time (0−90 min), samples were withdrawn and diluted 25- and 60-fold for free and TF-bound VIIa, respectively, into 0.7 mM Chromozym tPA to determine the amidolytic activity of the unreacted enzyme. Rates of inactivation were calculated from a plot of the residual activity versus the incubation time.

Determination of the Functional Plasma Half-Life of VIIa. To analyze the time dependence of inhibition of VIIa in plasma, citrated plasma was recalcified with 30 mM $CaCl_2$ in the presence of 1 μM Xa inhibitor NAP5 (Corvas International, San Diego, CA) and 2 μM thrombin inhibitor hirudin (Calbiochem, La Jolla, CA) to prevent clotting. The inhibition of 40 nM wild-type or mutant VIIa was assessed by incubation of the spiked human pool plasma at 37 °C. Samples were taken after 10−120 min and diluted into sTF (1 μM) and chromogenic substrate Chromozym tPA (0.7 mM) to determine the residual amidolytic activity. To calculate $t_{1/2}$, mean values of three experiments were fitted to an exponential decay equation using least-squares regression analysis.

Surface Plasmon Resonance Analysis. The kinetics of binding of wild-type and mutant VII/VIIa to TF were analyzed using a BIAcore 2000 instrument (Pharmacia Biosensor), as described previously (*12*). Briefly, full-length recombinant TF was injected to saturate a noninhibitory anti-TF antibody (TF9-10H10) directly immobilized by amino coupling to an activated dextran matrix. Association was monitored during injection of five concentrations (from 25 nM to 1 μM) of VII/VIIa in HBS, 5 mM $CaCl_2$, 0.005% surfactant P20, and 3 mM CHAPS. Dissociation data were collected for 250 s after a return to buffer flow, and the chip surface was regenerated with pulses of 0.1 M EDTA and 4 M $MgCl_2$. Association and dissociation constants (k_{on} and k_{off}, respectively) were determined using the software provided by the manufacturer.

Table 1: Sequence Alignment of Residues Determining Zymogenicity in Factor VIIa

	21	154 156
Human VII	IVGGK**V**C----------	AL**E**L**M**VLNVPR
Bovine VII	IVGGH**V**C----------	AR**K**L**M**VVLVPR
Mouse VII	IVGGN**V**C----------	AL**E**L**M**VLNVPR
Zebrafish VII	IVGGS**E**C----------	SR**L**L**R**RLLVPR
Human IX	IVGGE**D**A----------	AL**V**L**Q**YLRVPL
Porcine IX	IVGGE**N**A----------	AT**I**L**Q**YLKVPL
Human X	IVGGQ**E**C----------	ST**R**L**K**MLEVPY
Bovine X	IVGGR**D**C----------	SS**T**L**K**MLEVPY
Human thrombin	IVEGS**D**A----------	PS**V**L**Q**VVNLPI
Bovine thrombin	IVEGQ**D**A----------	PS**V**L**Q**VVNLPL

RESULTS

Mutational Analysis of the Residue Triad of Val[21], Glu[154], and Met[156]. The residue triad at the amino-terminal insertion site has unusual side chain properties compared to the properties of other homologous coagulation factors (Table 1). While individual Ala substitution of these residues resulted in considerably diminished proteolytic activity (*1*), several side chain combinations at these three positions were well-tolerated for VIIa function (Figure 2). The transient screening assay for the individual Gln replacement for Met^{156} reliably showed the established normal proteolytic activity and increased affinity for TF (*16*). Combination mutants of the three residue positions showed a complex cooperative effect on cofactor affinity and catalytic function. Most importantly, affinity for TF and proteolytic function were frequently influenced in opposite directions by these side chain combinations.

For example, individual substitution of the hydrophobic Val^{21} with Asp left the affinity for TF essentially unchanged, but considerably reduced proteolytic activity in comparison to that of wild-type VIIa. In contrast, Val^{21} to Asn mutation showed the same loss of proteolytic activity as the Asp mutation, but the affinity for TF was increased to an extent that was observed for $VIIa_{Q156}$. Remarkably, no loss of proteolytic function was observed when Gln^{156} was introduced simultaneously with either Asp^{21} or Asn^{21}, which is evidence for a cooperative effect of the two residue positions in the activation pocket.

Changing residue 154 to a hydrophobic Ile, Val, or Leu residue typically had a minor effect in comparison to the single or double mutations. However, in combination with Gln^{156}, Val^{154} increased the K_d for TF and somewhat decreased proteolytic activity. In triple mutants including Gln^{156}, Leu^{154} in combination with Asp^{21} predominantly influenced affinity, whereas Leu^{154} in combination with Asn^{21} primarily reduced proteolytic function. Thus, the cooperative effect of these mutations on TF affinity can be separated from influences on proteolytic function.

Enzymatic Activity of $VIIa_{N21I154Q156}$. Changing the hydrophobic Met^{156} to Gln already significantly improved catalytic function and increased the affinity for TF, without stabilizing the amino-terminal insertion (*16*). The transient screening demonstrated that additional substitution of residues 21 and

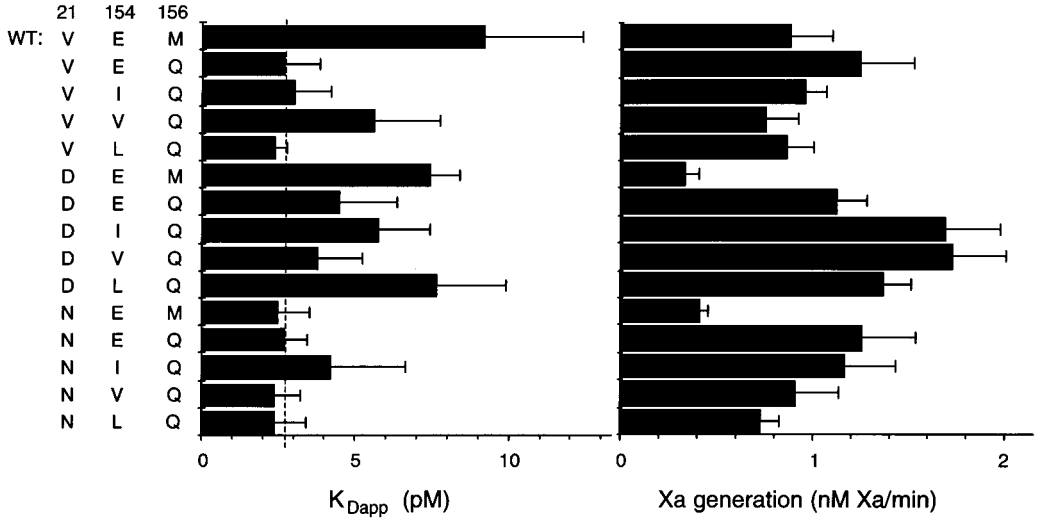

FIGURE 2: Characterization of VII variants by a functional assay. The affinity for phospholipid-reconstituted TF (left) and the rates for factor X activation (right) for the transiently expressed VII variants are shown. The dashed line marks the K_D of $VIIa_{Q156}$. The values are means ± standard deviations ($n = 7-12$).

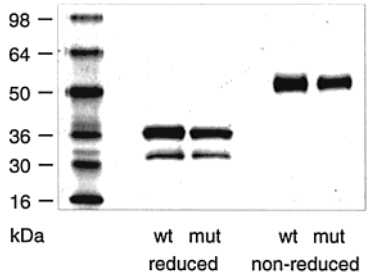

FIGURE 3: SDS−polyacrylamide gel electrophoresis of the protein after autoactivation. Wild-type VIIa (wt) or $VIIa_{N21I154Q156}$ (mut) was separated under reducing (left) or nonreducing (right) conditions and visualized by Coomasie blue staining. Nonreduced VIIa migrated with a mobility corresponding to the 50 kDa marker and the reduced heavy and light chains at 36 and 32 kDa, respectively.

Table 2: Proteolytic Function[a]

(A) Xa Generation by 20 nM Free VIIa

	Xa ($\times 10^{-2}$ nM/min)	
	VIIa	VIIa with PCPS
wild-type VIIa	0.5 ± 0.2	4.1 ± 0.1
$VIIa_{N21I154Q156}$	6.1 ± 0.9	53.8 ± 8.2

(B) Kinetic Parameters for X Activation in the Presence of Phospholipid-Reconstituted TF

	K_m (nM)	k_{cat} (s^{-1})	k_{cat}/K_m ($\times 10^8$ M^{-1} s^{-1})
wild-type VIIa	59 ± 4	11.9 ± 0.5	2.2 ± 0.2
$VIIa_{N21I154Q156}$	63 ± 4	14.1 ± 1.2	2.1 ± 0.1

[a] Values are means ± standard deviations ($n = 4$).

154 permits normal or enhanced function of the TF-bound VIIa. Because of its linear connectivity to the amino-terminal Ile^{16}, position 21 may contribute to the stabilization of the $Ile^{16}-Asp^{194}$ salt bridge in the context of the other mutations. We chose to further characterize the VIIa variant where the residue triad was converted to the counterparts of porcine factor IX ($VIIa_{N21I154Q156}$). The triple mutant was expressed by stable transfection of CHO cells and purified. Part of the protein was set aside to characterize the zymogen form, and the remaining VII was converted to the active enzyme by autoactivation. Autoactivation of the mutant occurred at a markedly faster rate than autoactivation of wild-type VII, suggesting increased catalytic activity. The mutant was fully activated after 24 h, whereas autoactivation of wild-type VII required 3 days in a parallel reaction. Electrophoretic analysis showed >95% conversion to the two-chain enzyme that was indistinguishable from wild-type VIIa and no apparent degradation of the protein (Figure 3).

Kinetic parameters for macromolecular substrate X activation by the TF−VIIa complex were similar for wild-type and mutant VIIa (Table 2). These data confirm the transient screening, which showed that the three side chain replacements did not perturb the function of TF-bound VIIa. When factor X activation by free VIIa was analyzed in the presence and absence of a negatively charged phospholipid surface (PCPS), the rate of Xa generation was ~9-fold higher in the presence of phospholipids for both wild-type and mutant VIIa. However, free $VIIa_{N21I154Q156}$ catalyzed X activation at a rate increased approximately 13-fold compared with that of wild-type VIIa, independent of the presence of phospholipids (Table 2). Thus, the mutations enhanced proteolytic function of the free mutant over wild-type VIIa, but there was only a modest <2-fold improvement relative to the single replacement mutant $VIIa_{Q156}$ (*16*).

Chromogenic substrate Chromozym tPA hydrolysis showed that the side chain replacements did not appreciably influence the amidolytic activity of the TF-bound VIIa. Nevertheless, the rate of substrate hydrolysis by the mutant in the absence of the cofactor was enhanced 7-fold compared to that of wild-type VIIa (Table 3). The free mutant displayed a k_{cat} that was close to the k_{cat} of TF-bound wild-type VIIa, thus clearly demonstrating an improved function relative to the individual $VIIa_{Q156}$ mutant (*16*). However, the K_m for Chromozym tPA cleavage by free $VIIa_{N21I154Q156}$ was only partially brought to the value of TF-bound wild-type VIIa. The affinity of the free mutant for the S1-occupying inhibitor *p*-aminobenzamidine was increased relative to that of free wild-type VIIa (Table 3), but did not reach the level of the TF−VIIa complex, arguing that the S1 subsite is only partly stabilized by the side chain replacements. The affinity for *p*-aminobenzamidine of TF-bound wild-type and mutant VIIa was similar, and the cofactor enhanced the catalytic efficiency

Table 3: Chromogenic Substrate Hydrolysis[a]

	K_m (mM)	k_{cat} (s^{-1})	k_{cat}/K_m ($\times 10^{-3}$ M^{-1} s^{-1})	K_i for *p*-amino-benzmidine (μM)
free				
wild-type VIIa	5.5 ± 0.4	8.4 ± 0.7	1.5 ± 0.1	~1000
$VIIa_{N21I154Q156}$	3.1 ± 0.6	32.2 ± 4.8	10.3 ± 0.4	317 ± 7
with sTF				
wild-type VIIa	0.8 ± 0.04	37.2 ± 3.1	46.2 ± 1.8	116 ± 17
$VIIa_{N21I154Q156}$	0.9 ± 0.07	47.0 ± 1.5	50.4 ± 2.8	124 ± 12

[a] Values are means ± standard deviations ($n = 3$).

of the mutant by approximately 5-fold, yielding essentially identical k_{cat}/K_m values for mutant and wild-type VIIa when bound to TF (Table 3). The incomplete maturation of the S1 subsite in free $VIIa_{N21I154Q156}$ may indicate that TF produces allosteric effects unrelated to the insertion site. In part, these may involve a previously characterized conformational network involving the buried Phe^{225} residue (*26*).

Increased Stability of the Amino-Terminal Insertion. The stability of the Ile^{16}−Asp^{194} salt bridge was analyzed by measuring the susceptibility to modification by KNCO, which results in a loss of activity due to carbamylation of the α-amino group of Ile^{16} (*25*). TF-bound wild-type and mutant VIIa showed identical rates of inactivation by KNCO (0.9 ± 0.2% loss of initial activity in 10 min, $n = 4$), providing evidence that the mutations did not prevent amino-terminal insertion, as previously shown for loop exchange mutants in VIIa (*27*). Carbamylation of free $VIIa_{N21I154Q156}$ occurred at a rate that was slower than that of wild-type VIIa (1.9 ± 0.4 vs 5.4 ± 0.5% loss of initial activity in 10 min, $n = 4$), demonstrating that the amino-terminal insertion is significantly more stabilized in comparison to the single Gln^{156} mutant.

Increased TF Affinity of the Enzyme Form of $VIIa_{N21I154Q156}$. Consistent with the increased affinity for TF revealed by the transient screening assay (Figure 2), $VIIa_{N21I154Q156}$ (5 nM) was 4-fold more efficient than wild-type VIIa in macromolecular substrate X activation at subsaturating concentrations (5 nM) of soluble TF, whereas wild-type and mutant VIIa activated X similarly at saturating (1 μM) soluble TF (data not shown). The increased affinity of the mutant for TF may result from a destabilization of critical contacts that maintain the zymogen-like state of VIIa. The hydrogen bonding of the Glu^{154} side chain with the backbone of residues 21 and 22 in the zymogen structure suggests that this zymogenicity-determining residues may have a prominent function in stabilizing the zymogen-like conformation of VII. However, mutation of residues 21, 154, and 156 did not influence the association kinetics of either zymogen VII or enzyme VIIa (Table 4), consistent with previous analysis of $VIIa_{A154}$ (*28*) and $VIIa_{Q156}$ (*16*). The residues that determine the zymogen-like properties of VIIa have thus no role in preventing the association of VII or VIIa with TF, and the prominent features of the zymogen structure (*6*), including the distorted TF-binding helix, pose no major energetic barrier for assembly with TF.

Stabilization of the active enzyme conformation by occupancy of the S1 subsite with transition state analogue inhibitors decreases the rate of dissociation of VIIa from TF (*12*). This may be interpreted to indicate that even when bound to the cofactor, VIIa retains a flexibility that facilitates dissociation like the zymogen. A decreased rate of dissociation from TF characterized $VIIa_{Q156}$, and dissociation of this mutant was not affected by active site inhibition (*16*). This supports the notion that not active site occupancy per se but rather restricted conformational flexibility is a major determinant that regulates the dissociation from the cofactor. As compared to wild-type VIIa, $VIIa_{N21I154Q156}$ also dissociated much slower from TF. In contrast, the same side chain replacements had only a minor <2-fold effect on the dissociation rates of the zymogen form of this mutant (Table 4). Thus, disruption of the hydrogen bonds involving Glu^{154}, as seen in the zymogen structure, is not sufficient for tighter binding of the zymogen to TF. The requirement for zymogen conversion in revealing the mutational effect of $VIIa_{N21I154Q156}$ indicates that these mutations predominantly stabilize the activation pocket and thus the active enzyme conformation.

Table 4: Binding of VII/VIIa to TF_{1-263}[a]

	k_{on} ($\times 10^5$ M^{-1} s^{-1})	k_{off} ($\times 10^{-4}$ s^{-1})
enzyme		
wild-type VIIa	3.0 ± 0.2	7.4 ± 0.3
$VIIa_{N21I154Q156}$	2.1 ± 0.2	1.4 ± 0.1
zymogen		
wild-type VII	2.5 ± 0.1	5.3 ± 0.1
$VII_{N21I154Q156}$	2.4 ± 0.1	3.7 ± 0.1

[a] Values are means ± standard deviations ($n = 3$).

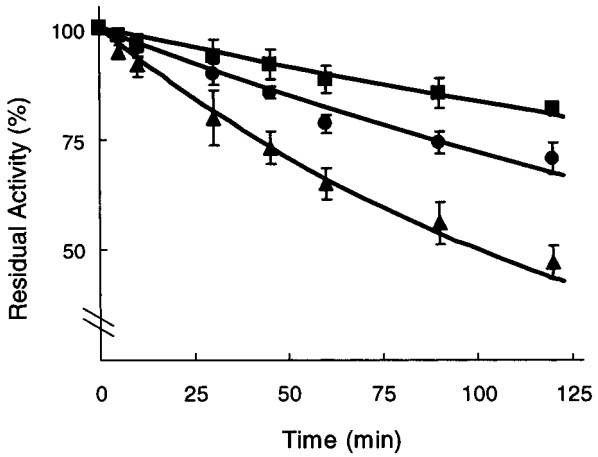

FIGURE 4: Inhibition of VIIa variants in plasma. Residual amidolytic activities of 40 nM wild-type VIIa (■), $VIIa_{Q156}$ (●), or $VIIa_{N21I154Q156}$ (▲) were determined after the indicated times of incubation in 200 μL of recalcified plasma at 37 °C. Clotting was prevented by the addition of the specific Xa inhibitor NAP5 (1 μM) and the thrombin inhibitor hirudin (2 μM). The values are means ± standard deviations of three experiments.

Effect of Mutations on Inhibition of VIIa Activity in Plasma. The Met^{156} to Gln mutation in VIIa has been shown to slightly increase the susceptibility to inhibition by antithrombin III (*16*). However, this increase was far smaller than the enhancement in the catalytic function of the free enzyme. The fact that VIIa circulates as an active enzyme is commonly assumed to originate from the zymogen-like properties, but this notion has not been tested experimentally. It was therefore of interest to examine the resistance to inhibition of VIIa mutants with a stabilized enzyme conformation. As shown in Figure 4, little inhibition was observed for wild-type VIIa and >80% of the initial amidolytic activity could be detected after incubation for 2 h at 37 °C.

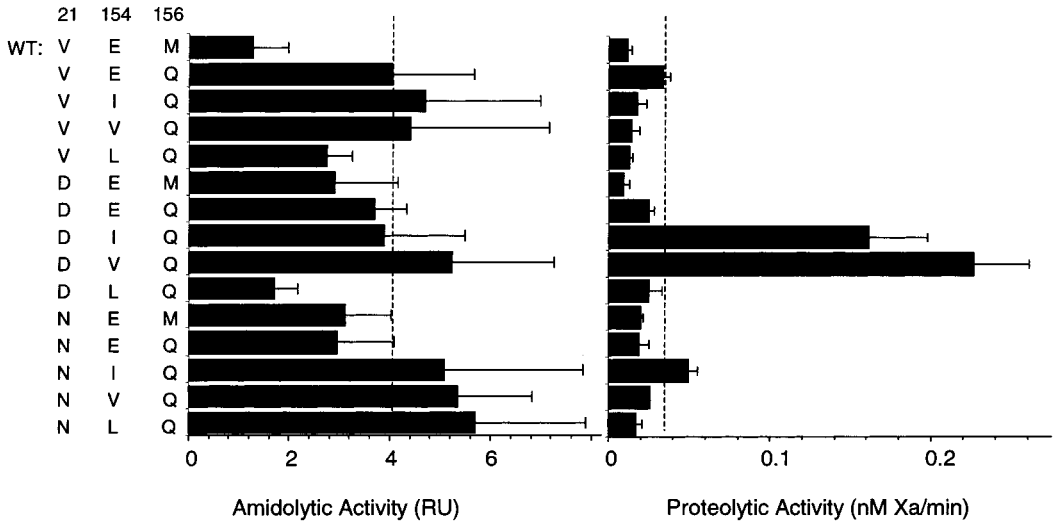

FIGURE 5: Catalytic activity of transiently expressed VIIa variants in the absence of TF. Hydrolysis of 0.7 mM Chromozym tPA by 5 nM VIIa was assessed at ambient temperature (left). Activation of X (1 μM) by 10 nM VIIa was assessed after incubation for 20 min at 37 °C (right). Dashed lines delineate the rates for $VIIa_{Q156}$. The values are means ± standard deviations ($n = 4-11$). RU represents relative absorbance units.

Whereas inhibition of $VIIa_{Q156}$ occurred at somewhat faster rates ($t_{1/2} = 211$ min for $VIIa_{Q156}$ vs 385 min for the wild type), the $VIIa_{N21I154Q156}$ mutant was much more rapidly inhibited, with 50% of the initial activity remaining after 101 min (Figure 4). Considering the modest improvement in amidolytic and proteolytic activity of the triple mutant compared with that of $VIIa_{Q156}$, these data suggest that the stabilized amino-terminal insertion is a significant factor that increases the susceptibility to inhibition in plasma.

Importance of the Charge Properties of the 21 Position in Macromolecular Substrate Recognition. The changes in the protection of the amino terminus of the $VIIa_{N21I154Q156}$ mutant and the ~2-fold increase in amidolytic activity relative to $VIIa_{Q156}$ were very similar to those of a recently described mutant, $VIIa_{D21V154Q156}$ (*17*), in which the residue triad was converted into a thrombin-mimicking sequence. However, a dramatic difference was observed in the proteolytic activity of the free enzymes. Whereas X activation of $VIIa_{N21I154Q156}$ was improved <2-fold relative to that of $VIIa_{Q156}$ (Table 2), $VIIa_{D21V154Q156}$ exhibited a 5.5-fold enhancement (*17*). These data suggest that amidolytic and proteolytic activities of free mutants were not strictly correlated. The effect of the various side chain combinations on amidolytic and proteolytic activity was therefore analyzed using transiently expressed mutants converted to enzyme VIIa.

Under these conditions, the rates of chromogenic substrate hydrolysis by free $VIIa_{Q156}$ or $VIIa_{N21I154Q156}$ and $VIIa_{D21V154Q156}$ were increased 3- or 5-fold, respectively, over that of wild-type VIIa (Figure 5), in reasonable agreement with data obtained using purified proteins (Table 3 and ref *17*). A large number of mutants shared the increased amidolytic activities of free $VIIa_{N21I154Q156}$ and $VIIa_{D21V154Q156}$. $VIIa_{D21L154Q156}$ stood out in that its activity was unchanged relative to that of wild-type VIIa, indicating that the enzyme conformation was not appreciably stabilized in this mutant combination. Leu^{154} was also the least active of the hydrophobic substitutions in other combination mutants.

The majority of the mutants displayed proteolytic activities only slightly greater than that of wild-type VIIa, but the proteolytic activity of $VIIa_{D21V154Q156}$ was increased 6-fold relative to that of $VIIa_{Q156}$, consistent with previous analysis with purified protein (*17*). All triple mutants with an Asn^{21} displayed free proteolytic activities only slightly above that of wild-type VIIa, with the above-characterized $VIIa_{N21I154Q156}$ exhibiting the highest proteolytic function. However, charge conversion at the 21 position upon Asp mutation increased the proteolytic activity of the same residue combinations, with the exception of $VIIa_{D21L154Q156}$ which presumably lacked a stabilized enzyme conformation (see the amidolytic assay). Once a stabilized enzyme conformation is achieved, a negatively charged residue at position 21 is thus sufficient to enhance the activation of X, resulting in the drastically increased proteolytic activity of free $VIIa_{D21I154Q156}$ and $VIIa_{D21V154Q156}$ relative to that of Asn substitutions.

DISCUSSION

Retaining VIIa in a zymogen-like conformation is one of the requirements for regulating the initiation of coagulation through the allosteric control of the cofactor and cell surface receptor TF. The unusual hydrophobic Met^{156} in the activation pocket of the VIIa protease domain is essential for the zymogen-like properties of VIIa (*16*). However, changing Met^{156} did not stabilize the amino-terminal $Ile^{16}-Asp^{194}$ salt bridge, a hallmark of the active conformation of serine protease domains. That both $VIIa_{N21I154Q156}$ and the recently characterized $VIIa_{D21V154Q156}$ (*17*) show a stabilized amino-terminal insertion provides conclusive evidence that the atypical side chain properties of the 21, 154, and 156 positions locally control the crucial aspects of the zymogen-like state of free VIIa.

A consequence of the improved stabilization of the amino-terminal insertion was a drastically reduced survival of VIIa's activity in a plasma milieu. The zymogen-like properties of the VIIa protease domain thus endow the initiating protease of the coagulation cascade with a prolonged plasma half-life as an active enzyme by escaping plasma inhibitors. Interestingly, the side chain characteristics of the zymogenicity-determining triad in VIIa are well-conserved among

mammalian species, while in lower vertebrates, for example, in zebrafish, VIIa significantly differs in this region (Table 1). Zebrafish VIIa also displays structural divergences from mammalian counterparts in the 170 loop and in the TF contact residue Met^{164} (*30*), indicating that the cofactor interactions in zebrafish are significantly different from those in mammals. The allosteric control of the zymogen-like properties of VIIa has thus evolved specific features in warm-blooded mammals.

Changing the zymogenicity-determining residues to side chains of homologous proteases produced cooperative effects that stabilized a more active enzyme conformation and increased the affinity for TF. However, the effects on catalytic function and TF affinity were not strictly correlated, suggesting a complex allosteric role of these residues in the activation pocket of VIIa. $VIIa_{Q156}$ already showed a significantly reduced rate of dissociation from TF, and there was no additional decrease in the dissociation rate when the amino-terminal insertion was further stabilized by the mutations in $VIIa_{N21I154Q156}$. This finding expands on previous conclusions that the allosteric effects in the VIIa protease domain are discrete and not globally coupled (*3*).

The effect of the Gln^{156} mutation on dissociation from TF was equivalent to the effect of S1 subsite-occupying inhibitors in wild-type VIIa, and $VIIa_{Q156}$ did no longer respond to active site modification. However, the affinity for S1 subsite inhibitors and for chromogenic substrates was reduced in the case of free $VIIa_{N21I154Q156}$, suggesting that the slower dissociation from TF is improbably due to an indirect effect of a stabilized Asp^{189}. More likely, the mutations in the activation pocket influence the β-strand network, which connects to the crucial Met^{164} that is the target of the effect of active site modifications (*12*). The increase in affinity for TF was not observed in the zymogen form of $VIIa_{N21I154Q156}$, indicating that a stabilization of the enzyme conformation, rather than the disruption of the hydrogen-bonding network of Glu^{154}, which possibly stabilizes the conformation of the known zymogen structure (*6*), is responsible for the increased cofactor affinity.

The most significant finding was the discordant mutational effect on the enhancement of amidolytic and proteolytic activities of the free VIIa variants. Although position 154 has been discussed as the crucial residue side chain that enhances proteolytic function of combination mutants (*17*), our data clearly show that the charge property of position 21 is the relevant feature. Mutants with either Val or Ile at position 154 exhibit the same dramatic increase in the level of X activation when Asn in position 21 is converted to Asp. Because the amidolytic activities of these mutants were not appreciably influenced by the charge conversion, these data support the notion that the activation pocket is directly involved in an exosite that recognizes macromolecular substrate X. Consistently, a monoclonal antibody that covers the activation pocket has been previously shown to act as a competitive inhibitor of X activation by the TF−VIIa complex (*29*). Notably, enhanced activation of X by Asp^{21} mutants was most pronounced with free VIIa, suggesting that additional exosite interactions of X with TF partially mask the improved binding of substrate X with the exosite at the amino-terminal insertion site.

VIIa is widely used as a pan-hemostatic agent in the treatment of bleeding episodes, and mutants with increased proteolytic activities have been discussed as an improvement for antihemophilic therapy (*17*) through a TF-independent pathway on platelets (*31*). However, the zymogen-like properties of VIIa likely contribute to the advantageous clinical profile of a sufficiently long circulatory half-life and minimal adverse side effects due to nonspecific proteolysis. The reduced plasma survival of $VIIa_{N21I154Q156}$ suggests that highly active VIIa variants may face pharmacokinetic disadvantages that limit their use in antihemophilic therapy. Since it is incompletely understood whether the hemostatic effects of VIIa therapy are TF-dependent or TF-independent, VIIa mutants that have increased affinity for TF may prove to be useful in testing the importance of TF in the antihemophilic action of VIIa administration.

ACKNOWLEDGMENT

We thank Jennifer Royce, Cindi Biazak, Pablito Tejada, and Dave Revak for their assistance in the production and purification of recombinant proteins.

REFERENCES

1. Dickinson, C. D., Kelly, C. R., and Ruf, W. (1996) *Proc. Natl. Acad. Sci. U.S.A. 93*, 14379−14384.
2. Schechter, I., and Berger, A. (1967) *Biochem. Biophys. Res. Commun. 27*, 157−162.
3. Ruf, W., and Dickinson, C. D. (1998) *Trends Cardiovasc. Med. 8*, 350−356.
4. Huber, R., and Bode, W. (1978) *Acc. Chem. Res. 11*, 114−122.
5. Higashi, S., Matsumoto, N., and Iwanaga, S. (1996) *J. Biol. Chem. 271*, 26569−26574.
6. Eigenbrot, C., Kirchhofer, D., Dennis, M. S., Santell, L., Lazarus, R. A., Stamos, J., and Ultsch, M. H. (2001) *Structure 9*, 627−636.
7. Pike, A. C. W., Brzozowski, A. M., Roberts, S. M., Olsen, O. H., and Persson, E. (1999) *Proc. Natl. Acad. Sci. U.S.A. 96*, 8925−8930.
8. Johnson, D. J. D., Nugent, P. G., Tuddenham, E. G. D., Harlos, K., and Kemball-Cook, G. (1999) *J. Struct. Biol. 125*, 90−93.
9. Dennis, M. S., Eigenbrot, C., Skelton, N. J., Ultsch, M. H., Santell, L., Dwyer, M. A., O'Connell, M. P., and Lazarus, R. A. (2000) *Nature 404*, 465−470.
10. Banner, D. W., D'Arcy, A., Chène, C., Winkler, F. K., Guha, A., Konigsberg, W. H., Nemerson, Y., and Kirchhofer, D. (1996) *Nature 380*, 41−46.
11. Zhang, E., St. Charles, R., and Tulinsky, A. (1999) *J. Mol. Biol. 285*, 2089−2104.
12. Dickinson, C. D., and Ruf, W. (1997) *J. Biol. Chem. 272*, 19875−19879.
13. Broze, G. J. (1982) *J. Clin. Invest. 70*, 526−535.
14. Sakai, T., Lund-Hansen, T., Paborsky, L., Pedersen, A. H., and Kisiel, W. (1989) *J. Biol. Chem. 264*, 9980−9988.
15. O'Brien, D. P., Kemball-Cook, G., Hutchinson, A. M., Martin, D. M. A., Johnson, D. J. D., Byfield, P. G. H., Takamiya, O., Tuddenham, E. G. D., and McVey, J. H. (1994) *Biochemistry 33*, 14162−14169.
16. Petrovan, R. J., and Ruf, W. (2001) *J. Biol. Chem. 276*, 6616−6620.
17. Persson, E., Kjalke, M., and Olsen, O. H. (2001) *Proc. Natl. Acad. Sci. U.S.A. 98*, 13583−13588.
18. Ruf, W. (1994) *Biochemistry 33*, 11631−11636.
19. Ruf, W., and Edgington, T. S. (1991) *Proc. Natl. Acad. Sci. U.S.A. 88*, 8430−8434.
20. Carson, S. D., and Konigsberg, W. H. (1980) *Science 208*, 307−309.
21. Bach, R., Gentry, R., and Nemerson, Y. (1986) *Biochemistry 25*, 4007−4020.
22. Stone, M. J., Ruf, W., Miles, D. J., Edgington, T. S., and Wright, P. E. (1995) *Biochem. J. 310*, 605−614.
23. Fair, D. S., Plow, E. F., and Edgington, T. S. (1979) *J. Clin. Invest. 64*, 884−894.

24. Shobe, J., Dickinson, C. D., and Ruf, W. (1999) *Biochemistry 38*, 2745−2751.
25. Higashi, S., Nishimura, H., Aita, K., and Iwanaga, S. (1994) *J. Biol. Chem. 269*, 18891−18898.
26. Petrovan, R. J., and Ruf, W. (2000) *Biochemistry 39*, 14457−14463.
27. Soejima, K., Mizuguchi, J., Yuguchi, M., Nakagaki, T., Higashi, S., and Iwanaga, S. (2001) *J. Biol. Chem. 276*, 17229−17235.
28. Ruf, W., Shobe, J., Rao, S. M., Dickinson, C. D., Olson, A., and Edgington, T. S. (1999) *Biochemistry 38*, 1957−1966.
29. Dickinson, C. D., Shobe, J., and Ruf, W. (1998) *J. Mol. Biol. 277*, 959−971.
30. Sheehan, J., Templer, M., Gregory, M., Hanumanthaiah, R., Troyer, D., Phan, T., Thankavel, B., and Jagadeeswaran, P. (2001) *Proc. Natl. Acad. Sci. U.S.A. 98*, 8768−8773.
31. Hoffman, M., Monroe, D. M., and Roberts, H. R. (1998) *Blood Coagulation Fibrinolysis 9*, S61−S65.

BI0202169